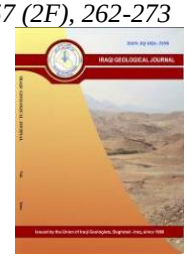
Iraqi Geological Journal

Journal homepage: https://www.igj-iraq.org



Noise Ratio Variation Effects on Visualizing Subsurface Targets in Electrical Resistivity Imaging (ERI) Sections

Raad Eissa[1,*]

[1] Department of Civil Engineering, College of Engineering, University of Kerbala, Karbala, 56001, Iraq
[*] Correspondence: raad.m@uokerbala.edu.iq

Received:
1 August 2024

Accepted:
1 September 2024

Published:
31 December 2024

Abstract

Geoelectrical methods, such as electrical resistivity, are frequently applied for indirect site investigations. The collected data might be affected by noise, overestimating, or underestimating the measurements. Noise affects electrical resistivity data, which is required to be determined. As a result, synthetic electrical resistivity data sets were numerically created using the RES2DMOD software, with experimental noise levels of 1%, 2%, 3%, and 4%. After that, the data sets were inverted using the RES2DINV software package, which included a robust algorithm. These datasets were generated by applying the dipole-dipole, Wenner, and Wenner-Schlumberger arrays for a geological model (a normal fault) and a geotechnical model (i.e., several subsurface targets). A qualitative comparison reveals that the performance of the dipole-dipole array was the best, and the array shows less effects of the noise on the electrical resistivity model. The Wenner-Schlumberger was on the second rank. In addition, the RMSE error values indicate an increase with the progress of the inversion process.

Keywords: Dipole-dipole; Noisy data; Site investigation; Wenner array

1. Introduction

The electrical resistivity method is frequently applied among other geophysical methods for shallow investigations and has been utilized for different purposes. It has been applied to a wide range of geotechnical site investigation studies (Eissa et al., 2019; Hojat et al., 2020; Ahmad et al., 2022; Dafalla and Alfouzan, 2023; Farias et al., 2023; Massinai et al. 2023); for sustainability studies (Jayawickreme et al. 2014). Due to the wide applications of the method, it has also been reviewed for several research topics, for soil sciences (Samouëlian et al. 2005), landslide investigations (Perrone et al. 2014), buried foundations (Eissa, 2021), and for concrete durability (Azarsa and Gupta, 2017). Furthermore, the resistivity surveys are cost-effective, fast, and preliminary results can be obtained even in the site (McCann et al., 1997).

The electrical resistivity method can be deployed by so-called electrode arrays where four metal electrodes should generally be used (Keary et al., 2002). Szalai and Szarka (2008) summarized more than 100 electrode arrays based on the electrode arrangement; however, Wenner, dipole-dipole, and Wenner-Schlumberger are the most popular (Zhou and Dahlin, 2003). Two of the four electrodes are used for electrical current injection and the other two are used to measure potential difference values. The electrode for current injection is named C1 for the first one and C2 for the second one, while the electrode for potential difference measuring is called P1 for the first and P2 for the second (Reynolds, 2011). These four electrodes are put in linear profiles on the ground surface with a certain distance between any two electrodes (named electrode spacing a), which should be increased gradually to

DOI: 10.46717/igj.57.2F.17ms-2024-12-27

investigate deeper (Fig. 1). With some certain arrays, the second current and the second potential electrodes should be placed at remote distances such as in pole-pole array (Loke, 2021).

The geometric factor is a variable dependent on the electrode configuration used in the apparent resistivity calculations. The Wenner array possesses a lesser geometric factor, whereas the dipole-dipole array exhibits a more significant geometric factor, according to Loke (2021).

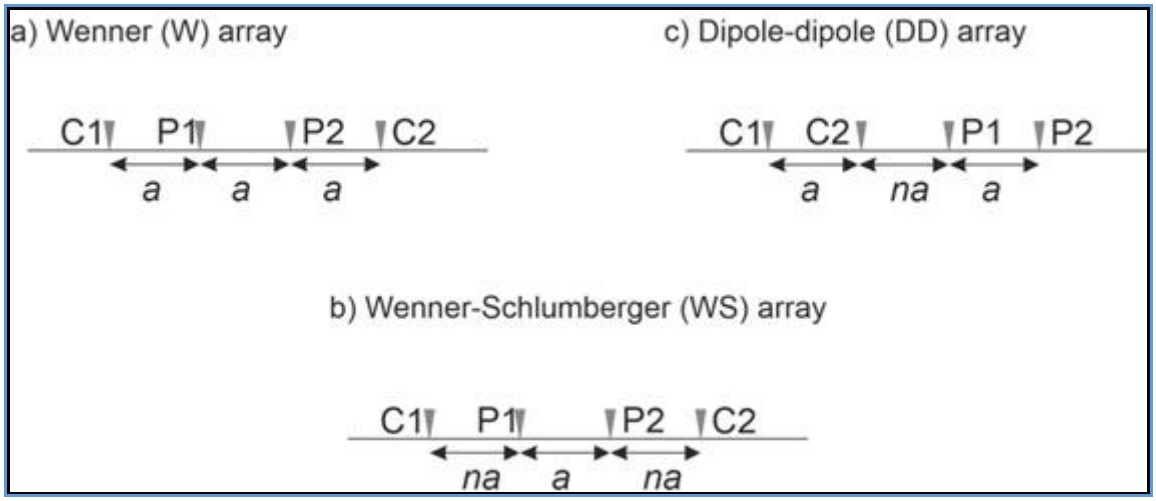


Fig. 1. Popular electrode array, a) Wenner array, b) Wenner-Schlumberger array, c) dipole-dipole array

Electrical resistivity data sets may be influenced by noise, leading to overestimating or underestimating anticipated resistivity readings (Keary et al., 2002). Noise can be categorized into two types: systematic noise, which arises from damage or malfunction of the survey equipment, and cable damage. The second type is random noise, which may originate from various sources, including telluric currents. Another cause may be the considerable distance between the remote electrodes, as observed in the pole-pole array (Loke, 2021). Resistivity measurements influenced by noise are termed bad data points.

Therefore, any gathered resistivity data set, before data processing, should be passed through a quality control check to eliminate any bad data point(s) (Loke, 2021). In some synthetic datasets studies, certain noise levels were added to the numerically generated data sets to mimic the possible noise effects in the field (Zhou and Dahlin, 2003; Eissa, 2022).

This study aims, therefore, to check the leverage of different noise values on the performance of some popular electrode arrays. However, the objectives are 1) to generate synthetic resistivity data sets using two models, a geological model represented by a normal fault and a geotechnical model represented by several subsurface targets, and 2) the synthetic models were created by anticipate dipole-dipole, Wenner, and Wenner-Schlumberger arrays, 3) adding different noise levels, 1%, 2%, 3%, and 4%, to simulate different field situations, 4) to process (i.e. applying the inversion process) all the prepared data sets, and finally 5) to compare the obtained resistivity models and to determine the best array's performance.

2. Methodology

Synthetic 2D electrical resistivity data sets were generated by the RES2DMOD software package, version 3.01. Electrode arrays of 61 electrodes were utilized with an electrode spacing of 1 m to generate a survey profile length of 60 m. Four nodes between any pair of electrodes were performed for better data resolution. Two groups of targets (i.e. proposed targets) were investigated using the finite element

algorithm (Loke and Barker, 1996): a geological model represented by a normal fault and another resistive buried target (Fig. 2 upper) and a geotechnical model represented by several underground anomalies which differ in their characteristics such as size, depth, and resistivity values (Fig. 2 lower). The geotechnical targets with resistivity values that were higher and lower than the hosting background were investigated in various underground scenarios. The conductive anomalies depict metallic objects and water-filled cavities, while the resistive anomalies represent resistive targets such as core stones, vacant cavities, and buried foundations. By performing the tested electrode arrays (Wenner, dipole-dipole, and Wenner-Schlumberger), these models were replicated.

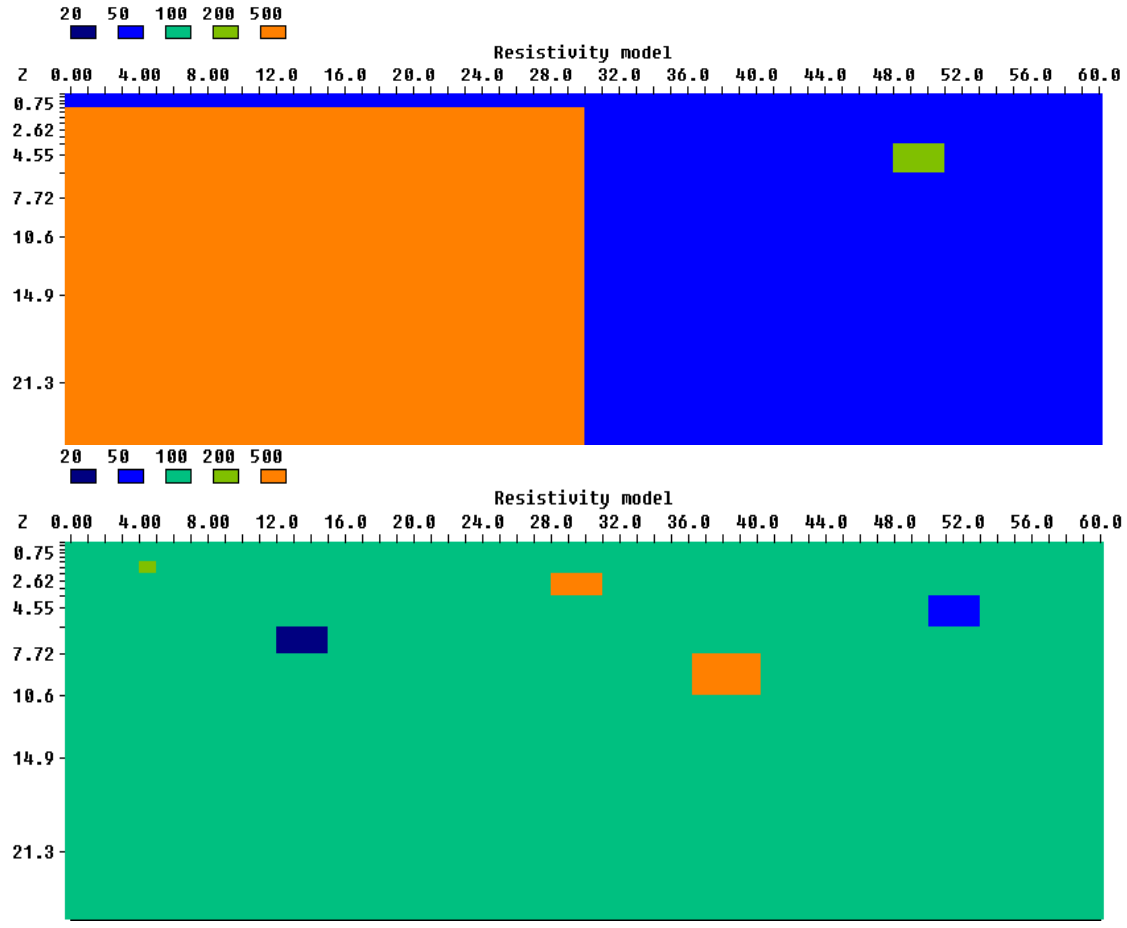


Fig. 2. Side views showing the investigated underground conditions obtained from the RES2DMOD, top: shows the normal fault geology, bottom: shows the geotechnical buried objects

Firstly, a standard dataset (zero noise) was generated for each investigated electrode array. After that, the data sets were regenerated by adding different noise values; 1%, 2%, 3% and 4% were chosen for comparison purposes.

3. Results and Discussion

The obtained 2D resistivity data sets were processed (i.e. the inversion process) by using the RES2DINV software package, version 4.08. The robust inversion algorithm had a robust data constraint cutoff factor of 0.05. However, the robust model constraint cutoff factor was 0.05.

3.1. Geological Model

Figs 3-5 show the obtained results for the geological model for all the investigated arrays (i.e. normal fault), where (a) refers to the model with no noise, b, c, d, and e refer to the 1%, 2%, 3% and 4% of noise, respectively. All the tested arrays reveal the location of the normal fault and the resistive target. In Fig. 3, on the dipole-dipole model, the deeper part of the normal fault is represented by wider resistivity contours, which indicates the limitation of the method in eliminating the deep parts of the target; however, adding noise to the dipole-dipole data sets does not show noticeable effects.

In the model from the Wenner array, as represented in Fig. 4, the normal fault is shown by wide resistivity contours, which is the poorest among the investigated arrays. Increasing the noise ratio slightly affects the fault appearance, where the resistivity contours get wider, even in the shallower parts of the fault. The array does not succeed in the reconstruction of the rectangular-shaped buried target.

For the Wenner-Schlumberger array applied, the fault is determined clearer at the top compared with the bottom parts, the same as the dipole-dipole array. However, adding noise makes the fault plane appear by wider resistivity contours, which ultimately adds more ambiguity to data interpretation (Fig. 5e). The array does not represent a response of the rectangular-shaped buried target.

Despite its original position, size, and shape, only the dipole-dipole array clearly shows the resistive rectangular-shaped buried target on the geological model. However, the Wenner and the Wenner-Schlumberger arrays are the poorest.

The dipole-dipole array is the optimal electrode array in recognizing the geological model, even though different noise ratios were added.

The RMSE error values show an increase with a higher noise ratio, which indicates the effect of the added noise on the inversion process and, ultimately, might increase the uncertainty of the data interpretation (Fig. 6). In addition, all the investigated arrays show comparable RMSE values of the same added noise ratio.

3.2. The Geotechnical Model

The RMSE error values for each investigated electrode array show an increase with a higher noise ratio Fig. 7.

For the geotechnical model, as represented in **Error! Reference source not found.** through 10. A lthough the investigated electrode arrays detect the subsurface targets, it shows the targets bigger than their original size, especially the deeper targets (targets 2 and 4).

All the investigated targets are identified on the dipole-dipole models. The shallowest targets (1 and 3) are eliminated in a good match with the original position and size of the original rectangular geometry of the targets. The responses from targets 2 and 4 are represented in a much wider response compared with their original characteristics. The dipole-dipole array shows the investigated anomalies almost in the same way as the noise-free model, which indicates the good performance of the array even when different ratios of noise were added (**Error! Reference source not found.**), this confims the good p erformance of the array as other studies have found (Eissa, 2022; Eissa, 2024).

In **Error! Reference source not found.**, the models from the Wenner array are represented. T argets number 3 and number 4 are combined on the same response on the noise-free model and the models with 1% and 2% of noise (**Error! Reference source not found.** b and c). Adding more noise (3% and 4%) makes the target number 4 (the deepest target) unidentified for the Wenner array (**Error! Reference source not found.** d and e). That can be related to the ambiguity of the resistivity method in determining deeper anomalies. In addition, target number 1 is unidentified with 4% noise (**Error! R eference source not found.** d).

The Wenner-Schlumberger array shows target numbers 1 and 3 reasonably matching their original characteristics. However, targets 2 and 4 are represented in much larger responses. Adding more noise

(i.e. 1 % to 4%) makes the array less effective in eliminating these investigated targets; e.g. 3 and 4 are almost combined in the same resistivity anomaly. Other targets are represented in the same way as in the noise-free model (Fig. 10).

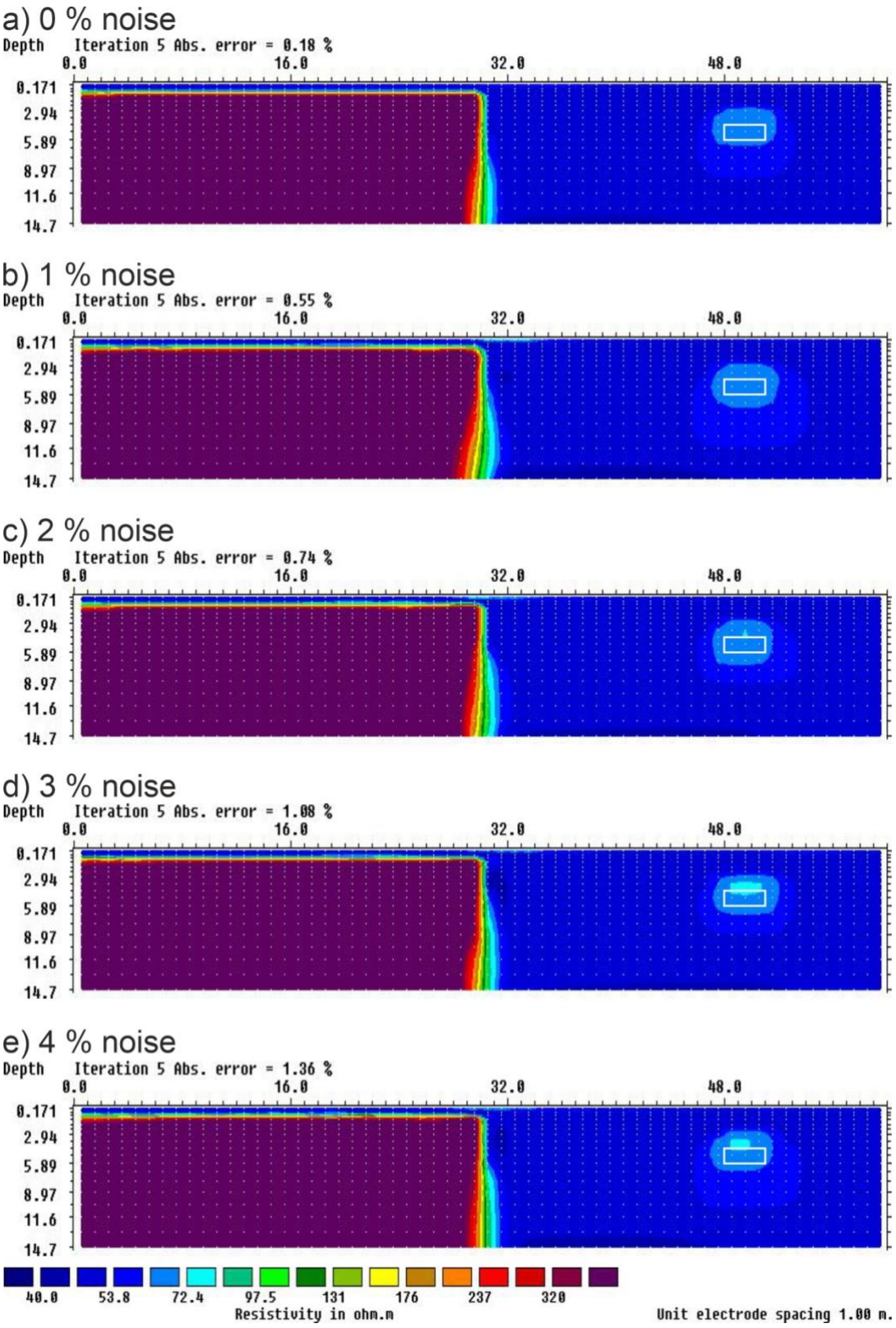


Fig. 3. Electrical resistivity response of the dipole-dipole array obtained to the geotechnical targets, the white rectangle shows the location of the target

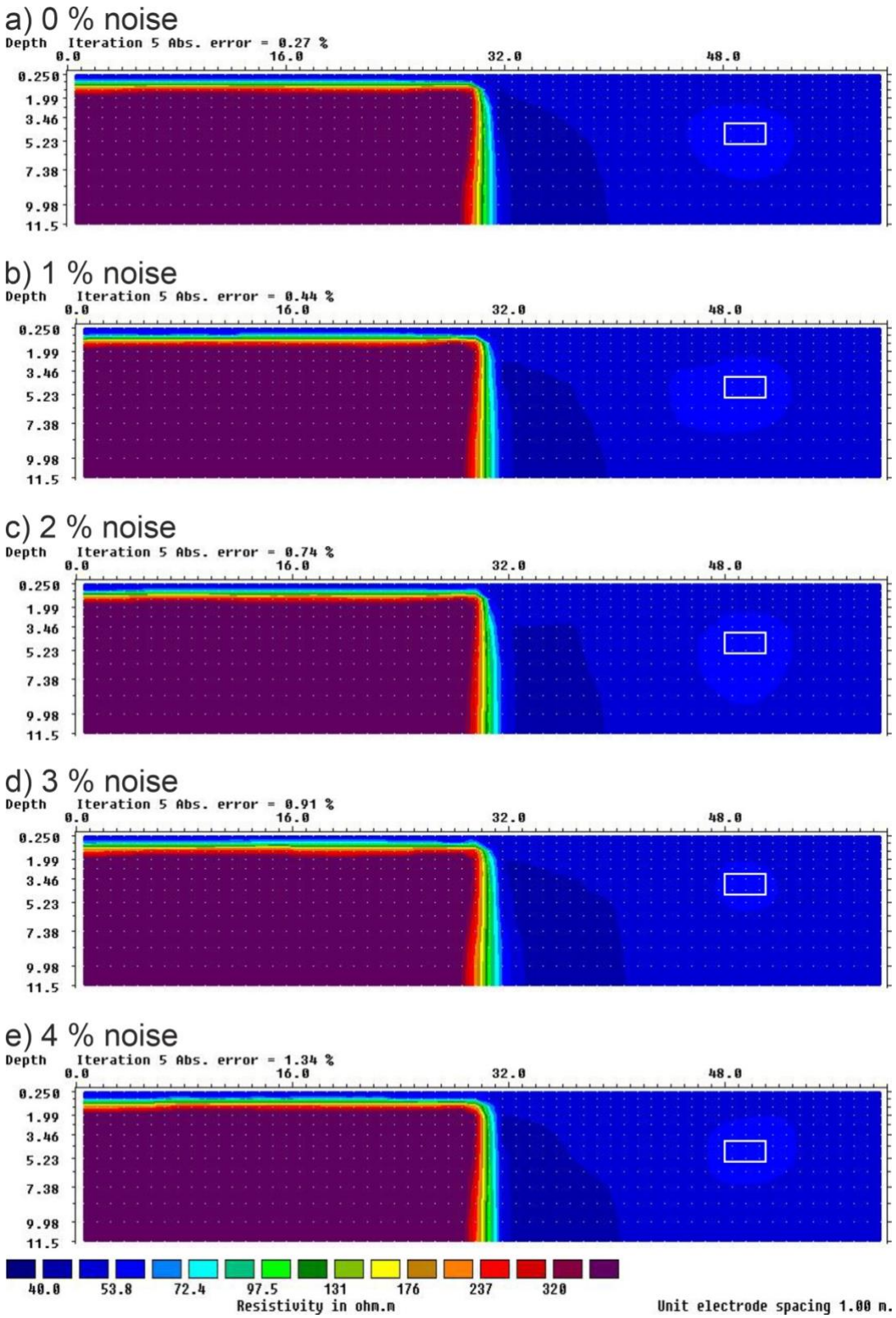


Fig. 4. Electrical resistivity response of the Wenner array obtained to the geotechnical targets, the white rectangle shows the location of the target

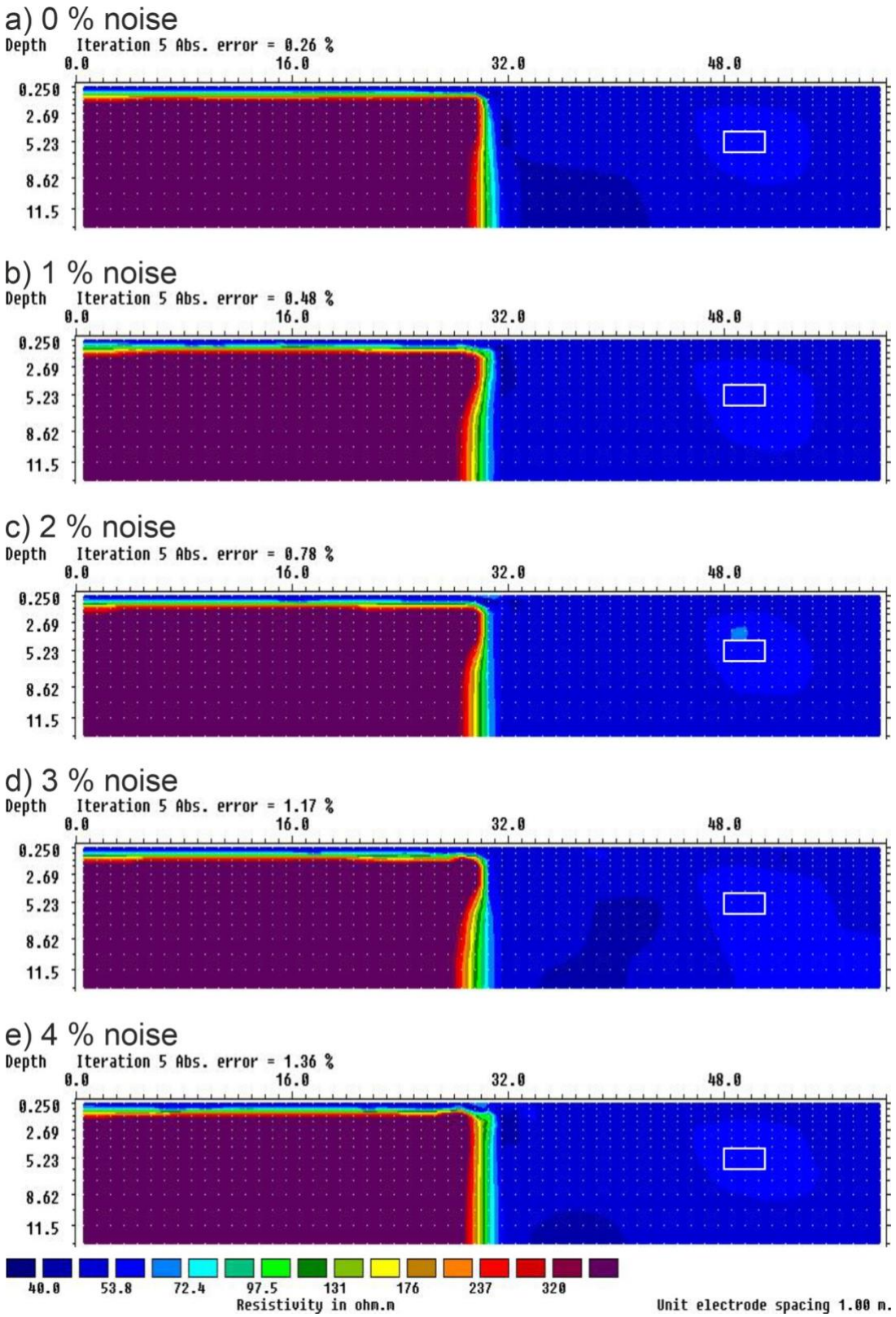


Fig. 5. Electrical resistivity response of the Wenner-Schlumberger array obtained to the geotechnical targets, the white rectangle shows the location of the target

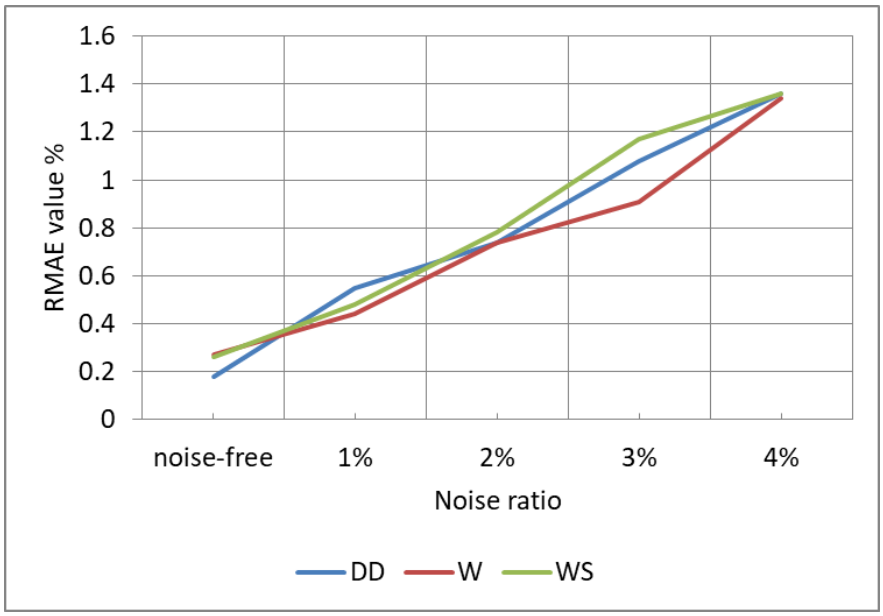


Fig. 6. The RMSE error values of the geological model obtained for the investigated arrays where DD refers to the dipole-dipole, W refers to the Wenner, and WS refers to the Wenner-Schlumberger array, shows a proportional relationship between noise ratio and RMAE

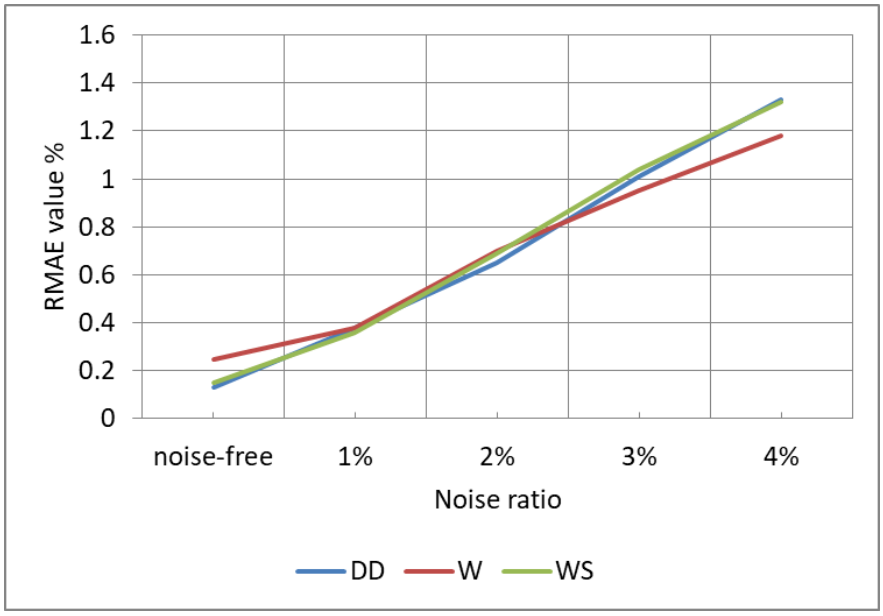


Fig. 7. This increase in the RMSE values indicates the effects of the added noise on the quality of the resistivity dataset and the difficulty in delivering sound interpretation. All the examined electrode arrays show a comparable and steady increase in the RMSE value

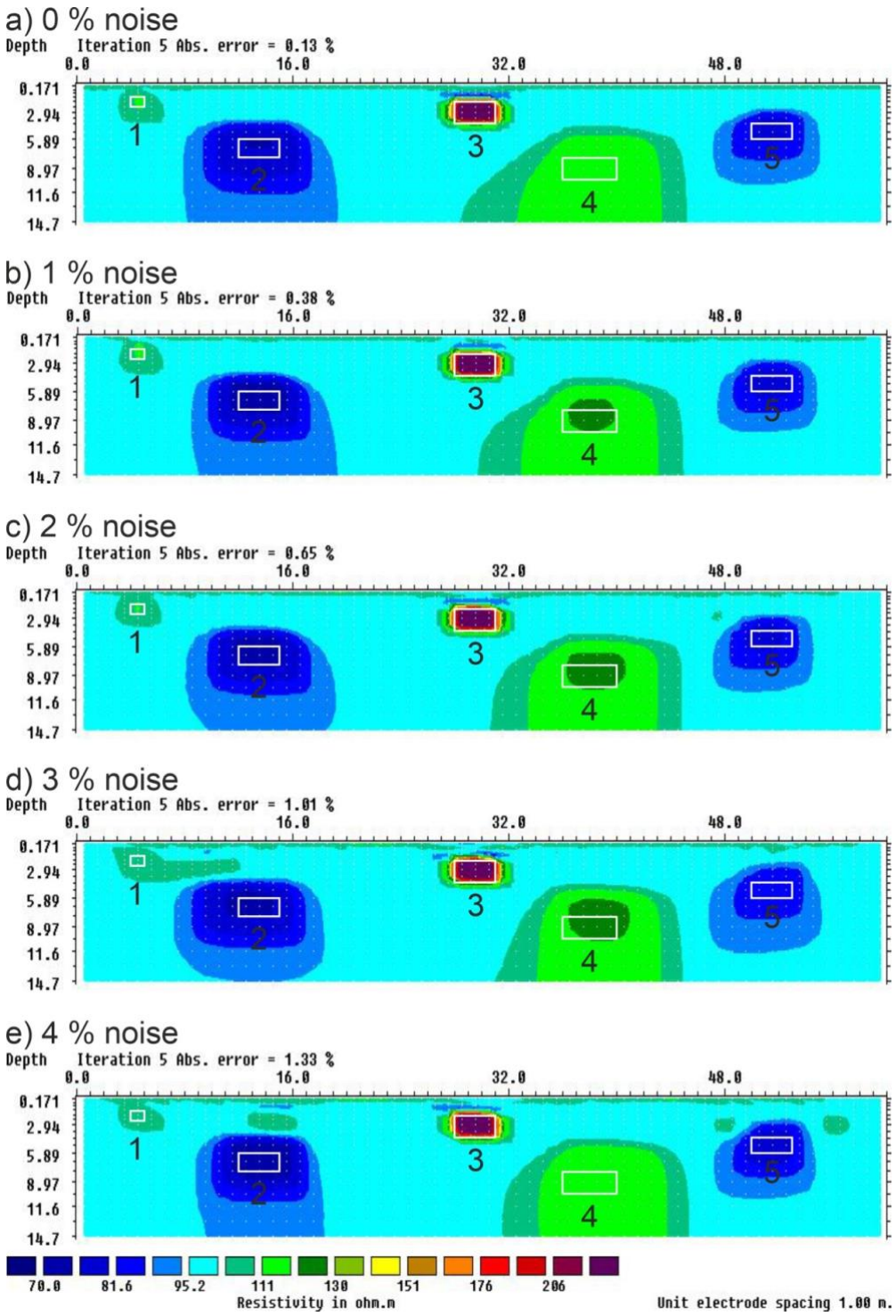


Fig. 8. Electrical resistivity response of the dipole-dipole array obtained to the geotechnical targets; the white rectangles show the location of the targets

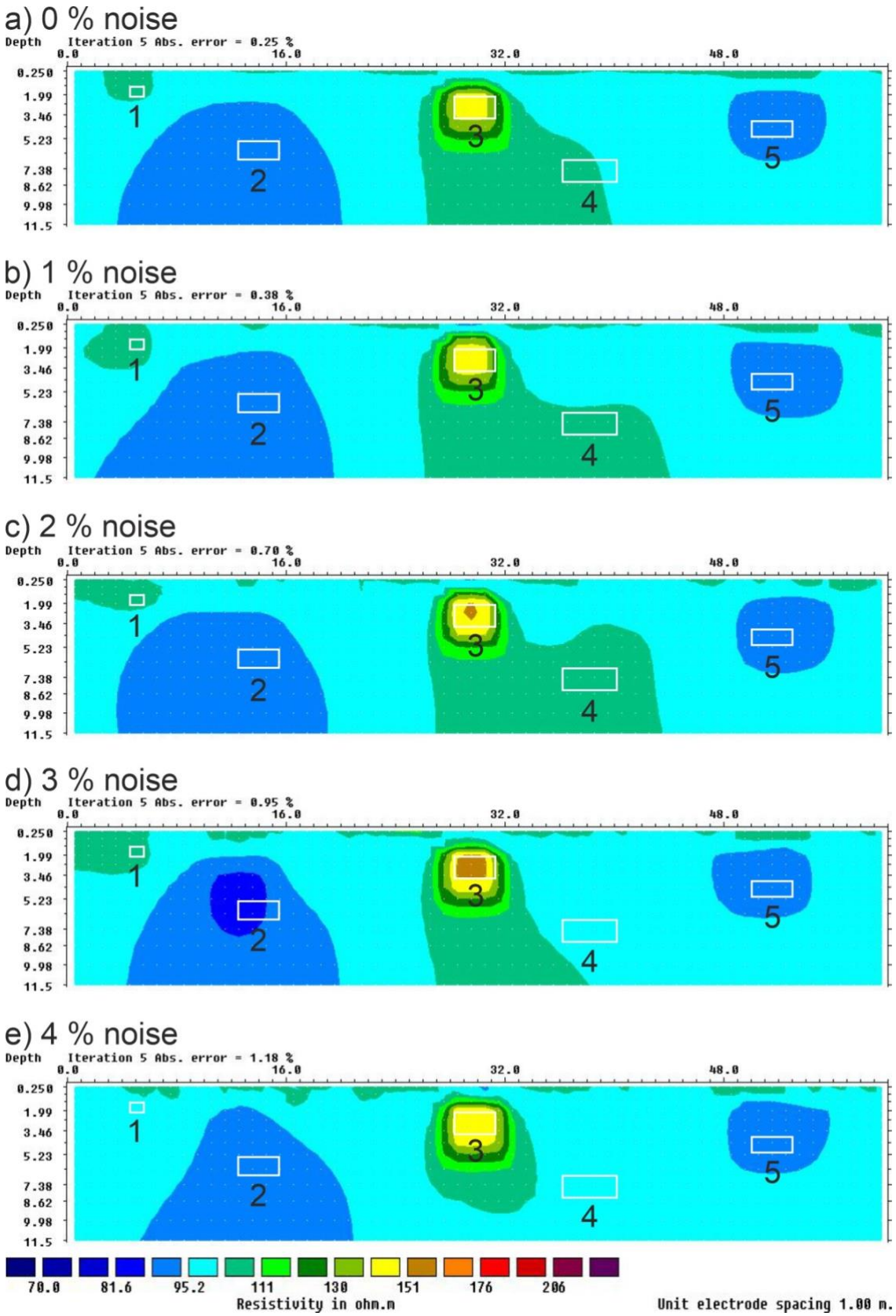


Fig. 9. Electrical resistivity response of the Wenner array obtained to the geotechnical targets, the white rectangles show the location of the targets

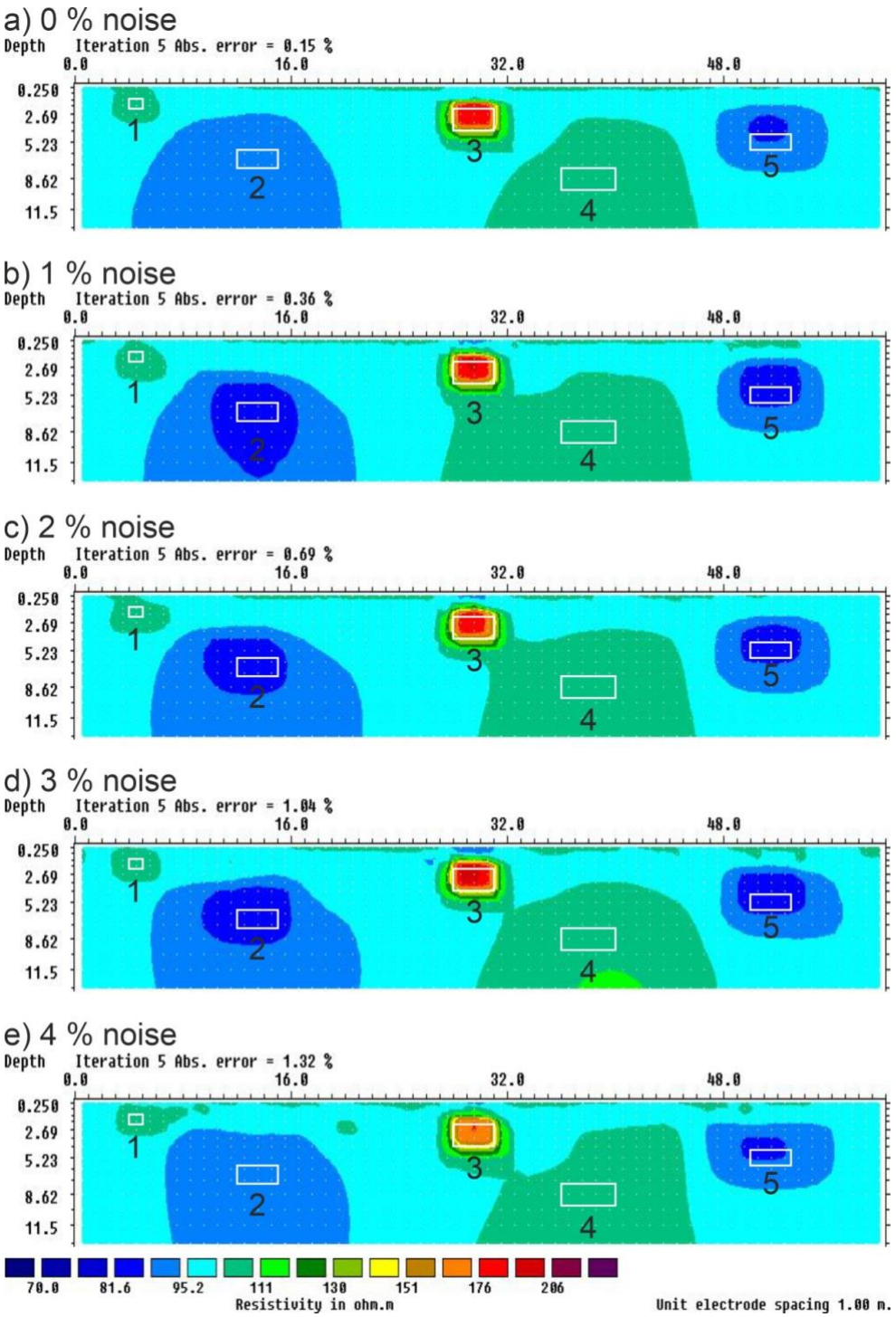


Fig. 10. Electrical resistivity response of the Wenner-Schlumberger array obtained to the geotechnical targets, the white rectangles show the location of the targets

4. Conclusions

Electrical resistivity data sets were created for geological and geotechnical models utilizing dipole-dipole, Wenner, and Wenner-Schlumberger arrays. Various noise level values (1%, 2%, 3%, and 4%) were applied to the resulting data sets. The generated electrical resistivity models were qualitatively compared after inverting the data with RES2DINV and the robust inversion algorithm. Increasing the noise in numerical studies reduces the arrays' effectiveness in eliminating subsurface characteristics and

increases the ambiguity of the data interpretation process. However, the dipole-dipole array provides the best model and reduces the impact of extra noise. A persistent increase in RMSE values was seen, contradicting the fundamentals of the inversion process. Implementing diverse electrode arrays offers the advantage of identifying their best performance in heterogeneous settings and noisy data interpretation.

References

Ahmad, W., Rehman, K., Farooq, M., Ali, A., Ahmed, T., 2022. Near-surface cavities mapping using integrated geophysical techniques: Case study of Gadwalian dam, North Pakistan. Iranian Journal of Earth Sciences, 14, 165–177.

Azarsa, P., Gupta, R., 2017. Electrical resistivity of concrete for durability evaluation: A review. Advances in Materials Science and Engineering, 1-30

Dafalla, M., Alfouzan, F., 2023. Electrical resistivity tomography of a gypsiferous subsurface soil: Geotechnical detection of a geoenvironmental phenomenon. Journal of King Saud University, 35,102595.

Eissa, R., 2022. Identification of different shallow foundations using 3D electrical resistivity modeling. Iraqi Geological Journal, 55, 111–120.

Eissa, R., 2021. Electrical resistivity tomography application for buried foundation investigations: Insights and review. Iraqi Geological Journal, 54, 122–133.

Eissa, R., Cassidy, N., Pringle, J., Stimpson, I., 2019. Electrical resistivity tomography array comparisons to detect cleared-wall foundations in brownfield sites. Quarterly Journal of Engineering Geoleology and Hydrogeology, 53, 137–144.

Eissa, R., 2024. The practicality of resistivity method for recognizing vertically distributed anomalies using simulated models. Iraqi Geological Journal, 57, 204-213.

Farias, ÉS., Machado, S.L., Giacheti, H.L., 2023. Site characterization and water content estimative. Soils and Rocks, 46, 1–10.

Hojat, A., Arosio, D., Ivanov, V.I., Loke, M.H., Longoni, L., Papini, M., Tresoldi, G., Zanzi, L., 2020. Quantifying seasonal 3D effects for a permanent electrical resistivity tomography monitoring system along the embankment of an irrigation canal. Near Surface Geophysics, 18, 427–443.

Jayawickreme, D.H., Jobbágy, E.G., Jackson, R.B., 2014. Geophysical subsurface imaging for ecological applications. New Phytologist, 201, 1170–1175.

Keary P., Brooks M., Hill I., 2002. An introduction to geophysical exploration, third ed. Blackwell science, 280.

Loke, M.H., 2021. Tutorial: 2D and 3D electrical imaging surveys, 1–176.

Loke, M.H., Barker, R.D., 1996. Rapid least-squares inversion of apparent resistivity pseudosections by a quasi-Newton method. Geophysical Prospecting, 44, 131–152.

Massinai, M.A., Massinai, M.F.I., Syamsuddin, E., 2023. Land subsidence assessment on karst based on resistivity and geotechnical parameters. Journal of Degraded and Mining Lands Management, 10, 4047–4059.

McCann, D.M., Culshaw, M.G., Fenning, P.J., 1997. Setting the standard for geophysical surveys in site investigation. Geological Society Engineering Geology Special Publication, 12, 2–32.

Perrone, A., Lapenna, V., Piscitelli, S., 2014. Electrical resistivity tomography technique for landslide investigation: A review. Earth-Science Reviews, 135, 65–82.

Reynolds, JM., 2011. An Introduction to Applied and Environmental Geophysics, second ed. Wiley-Blackwell, 696.

Samouëlian, A., Cousin, I., Tabbagh, A., Bruand, A., Richard, G., 2005. Electrical resistivity survey in soil science: A review. Soil Tillage Research, 83, 173–193.

Szalai, S., Szarka, L., 2008. On the classification of surface geoelectric arrays. Geophysical Prospecting, 56, 159–175.

Zhou, B., Dahlin, T., 2003. Properties and effects of measurement errors on 2D resistivity imaging surveying. Near Surfuce Geophysics, 1, 105–117.